Partial Oxidation of Ethane to Acetic Acid using a Metallic Pd Promoted MoVNb Catalyst Supported on Titania

[1]Sulaiman I. Al-Mayman*, [2]Abdulrahman S. Al-Awadi, [2,3]Yousef S. Al-Zeghayer and [4]Moustafa A. Soliman
[1]King Abdul Aziz City for Science and Technology, Riyadh, P.O. Box 6086, Riyadh 11442, Saudi Arabia.
[2]Department of Chemical Engineering, King Saud University, P.O. Box 800, Riyadh 11421, Saudi Arabia.
[3]Director of Industrial Catalysts Chair, King Saud University, P.O. Box 800, Riyadh 11421, Saudi Arabia.
[4]Chemical Engineering Department, Faculty of Engineering, The British University in Egypt, El-Sherouk City, Cairo, 11837, Egypt.
smayman@kacst.edu.sa**

(Received on 2nd January 2017, accepted in revised form 20th September 2017)

Summary: The partial oxidation of ethane to acetic acid on a multi-component $Mo_{16}V_{6.37}Nb_{2.05}Pd_x$ oxide catalyst supported on Degussa P25 titania has been investigated. The catalyst was characterized using BET surface area, X ray diffractometer (XRD) and transmission electron microscopy (TEM). The reaction was carried out in a differential reactor in a temperature range of 200-275°C and at a total pressure of 200 psi. The addition of trace amounts of nano-palladium, either as palladium oxides or metallic palladium, enhanced ethane oxidation towards the formation of acetic acid with near-complete depletion of the ethylene intermediate from the reactor effluent. The introduction of nano-Pd^0 to $Mo_{16}V_{6.37}Nb_{2.05}O_x/TiO_2$ decreased the required palladium source to a third when compared with nano-PdO_x. A green method was applied to prepare metallic nano-palladium using polyethylene glycol (PEG) and palladium acetate. PEG acted as a stabilizer and as a reducing agent. Transmission electron microscope (TEM) images of palladium nanoparticles showed an average size of approximately 15 nm. The as-prepared palladium nanoparticles were found to be highly stable.

Keywords: Ethane; Ethylene; Acetic acid; Metallic nano-palladium; Partial oxidation; MoVNbPd catalyst.

Introduction

Global acetic acid demand is steadily increasing due to the increase in the demand of its products: vinyl acetate monomer (VAM), purified terephthalic acid (PTA), ethyl acetate and acetic anhydride. Commercially, acetic acid is mainly produced from methanol carbonylation and acetaldehyde oxidation, which causes many problems such as corrosion and the disposal of environmentally unfriendly byproducts. Methanol carbonylation accounts for approximately 75% of the world capacity of acetic acid production. Direct oxidation of ethane and ethylene to acetic acid is an alternative that has shown promise [1, 2].

As an example, Showa Denko of Japan commercialized a process using palladium-based heteropoly acid catalysts for ethylene oxidation to acetic acid in 1997 [2]. A 30,000-ton/year acetic acid plant by ethane oxidation was commercialized by SABIC of Saudi Arabia in 2005. Selectivity of acetic acid from ethane oxidation as high as 80% can be obtained using a catalyst of mixture of Mo, V, Nb and Pd oxides. The main reaction equations describing the oxidation of ethane are:

$C_2H_6 + 1/2\ O_2 \rightarrow C_2H_4 + H_2O$ (1)
$C_2H_6 + 3/2\ O_2 \rightarrow CH_3COOH + H_2O$ (2)
$C_2H_6 + 5/2\ O_2 \rightarrow 2CO + 3H_2O$ (3)
$C_2H_6 + 7/2\ O_2 \rightarrow 2CO_2 + 3H_2O$ (4)

The product ethylene undergoes similar reactions:

$C_2H_4 + O_2 \rightarrow CH_3COOH$ (5)
$C_2H_4 + 2\ O_2 \rightarrow 2CO + 2H_2O$ (6)
$C_2H_4 + 3\ O_2 \rightarrow 2CO_2 + 2H_2O$ (7)

And acetic acid can be totally oxidized to CO andCO_2.

The study of a Mo-V-Nb catalyst for the partial oxidation of ethane to ethylene and acetic acid was pioneered in the works of Thorsteinson *et al.*. [1] and Young and Thorsteinson [3]. The use of high pressures and the addition of steam to the feed improved the selectivity to acetic acid. The process required a pressure of approximately 20 atm. The acetic acid selectivity was approximately 20%, and the ethylene selectivity was approximately 70%.

The addition of Pd increased selectivity to acetic acid to approximately 80% and completely oxidized CO to CO_2 as evidenced by the patents of Karim *et al.*. [4-6]. Borchert and Dingerdissen [7] reported a similar catalyst composition while Linke *et*

***To whom all correspondence should be addressed.**

al.. [8, 9] studied the mechanism and kinetics of the reaction. Another important finding is that of Li and Iglesia [10, 11] who found that the precipitation of a Mo, V, and Nb salts solution in the presence of colloidal TiO_2 (P25 titania from Degussa) led to a 10-fold increase in the ethylene and acetic acid oxidation rates (per active oxide) without significant changes in the selectivity relative to the unsupported samples. A mixture of 0.3 wt% Pd/SiO_2 was used to introduce trace amounts of Pd (0.0025–0.01 wt%); these trace amounts led to the near-complete depletion of ethylene and to a significant increase in the acetic acid synthesis rate. Al-Zaghayer *et al.*. [12] compared different grades of titania and concluded that P25 titania from Degussa gave the best performance.

In the last decade, palladium nanoparticles have been largely applied in catalysis by taking advantage of their metallic surface as well as their ability to generate molecular species. Because of their increased surface-to-volume ratios and their enhanced electronic properties from quantum confinement, nanoparticles often exhibit new or superior catalytic activities compared with their corresponding bulk materials. Nano-catalysis is becoming increasingly important as a means of producing more active and selective catalysts to counterbalance the increasing costs of energy and raw materials.

In the present study, we investigate the effect of adding metallic palladium nanoparticles on the performance of a supported Mo-V-Nb catalyst on titania for the partial oxidation of ethane.

Experimental

Catalyst Synthesis

Synthesis of Supported Mo-V-Nb-Pd oxide Catalyst

A Mo-V-Nb-Pd oxide catalyst was prepared using a wet impregnation method [4-6]. Three aqueous solutions were prepared: (1) 0.57 g ammonium m-vanadate was dissolved in 25 ml water while stirring and heating at 87°C. A yellow solution resulted. (2) 2.16 g ammonium p-molybdate was added into 20 ml water while stirring and heating at 60°C. A colorless solution resulted. (3) 0.97 g niobium oxalate (21.5% Nb_2O_5) was added into 20 ml water while stirring and heating at 63°C. A white solution formed. After each solution was stirred separately, 1.5 g oxalic acid powder was added gradually to the vanadate solution and stirred again at 87°C. Foam was observed during the addition of oxalic acid, but the foam bubbles burst quickly. The solution color changed from yellow to dark blue. The molybdate solution was then mixed with the previous solution and stirred again for 10 min at 87°C. Next, 5 g titania (Degussa P25, BET area: 54 m^2/g) was added to the mixture while stirring. The niobium oxalate solution was then added drop-wise, and Pd in the form of 10% oxidized Pd on charcoal was subsequently added. The mixture was stirred for an additional 10 min at 87°C. The water was evaporated, and the resulting paste was dried for 16 h at 120°C and calcined for 0.5 h at 350°C. This catalyst is denoted herein as $Mo_{16}V_{6.37}Nb_{2.05}$ Pd_i $/TiO_2$ with a catalyst loading of 30%.

Synthesis of Nano-metallic Palladium-containing Catalysts

Nano-Palladium Preparation

The nano-palladium preparation process is "green" and very simple [13, 14]. Polyethylene glycol (PEG) was used as both a stabilizer and a reducing agent. Palladium acetate (25 mg, 110 x 10^{-3} mmol) was added into PEG (molecular weight 4600, 2.0 g, 1.0 mmol) in a 50 ml round-bottom flask under vigorous stirring using a magnetic stirrer at 120°C. Palladium nanoparticles formed, as indicated by a dark-gray color. The mixture was further stirred for 2 h at the same temperature, and it solidified as it cooled to room temperature**.**

Mo-V-Nb-Pd /titania Synthesis

The as-prepared nano-metallic Pd was added to the solution containing the ammonium m-vanadate solution followed by the ammonium molybdate, titania and niobium oxalate solutions, as mentioned before.

Catalyst Characterization Techniques

The BET surface areas were measured using a Micromeritics ASAP2020 automated system with nitrogen adsorption-desorption at 77K. X-ray diffraction patterns of the catalysts and Pd nanoparticles were recorded using a Bruker D8 advance X-ray diffractometer using Cu-Kα radiation and a scan speed of 2.00 °/min. Transmission electron micrographs patterns were obtained with a Philips CM200 apparatus. Samples for TEM observation were prepared by placing 3 drops of the CH_2Cl_2 colloidal Pd/PEG solution onto a carbon-coated copper grid.

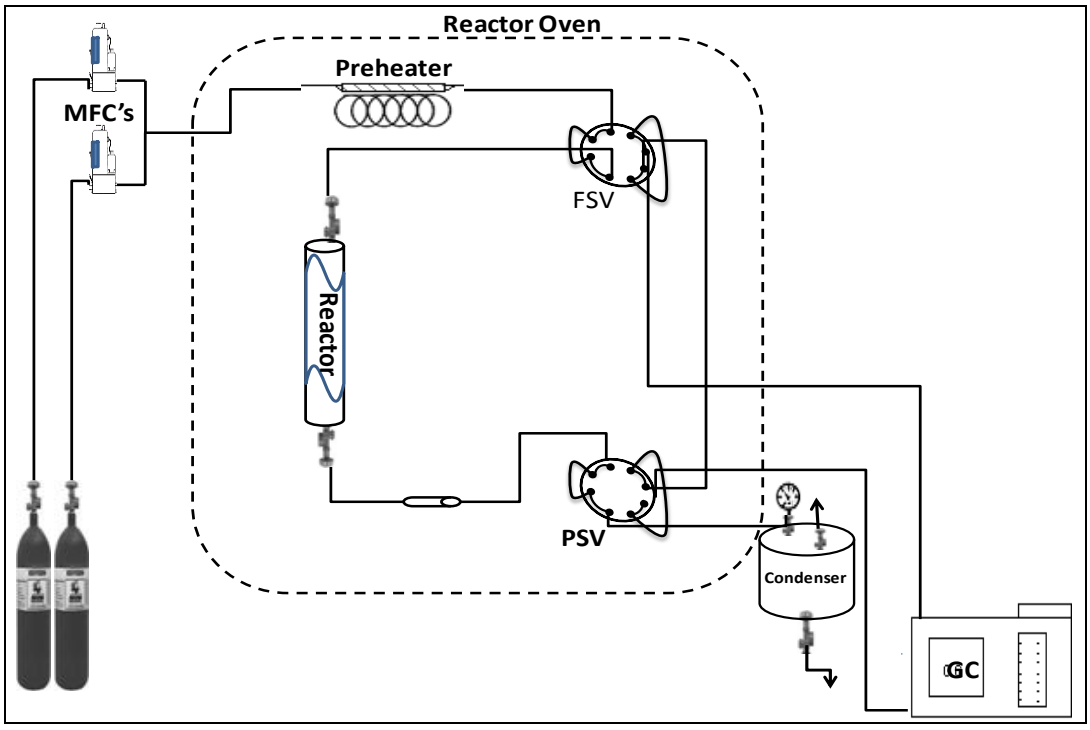

Fig. 1: A schematic of the experimental setup: MFCs: reactants' mass flow controllers, FSV: feed sample valve and PSV: products sample valve.

Catalyst Testing and Evaluation

The catalytic activities tests were performed at reaction temperatures of 225-275°C and a total pressure of 200 psi. The reactant flow rate was maintained at 15 ml/min (ethane and oxygen with volume percents of 82 and 18%, respectively) for a catalyst weight of 0.3 g. To avoid complete oxidation of ethane, oxygen is added in small percentage. The tests were carried out in an apparatus comprised of a reaction component and analysis component. As shown in Fig. (1), the reaction component mainly consisted of an oven and a reactor. The oven was a convection zone (a stainless steel box with the dimensions of 40 cm x 40 cm x 40 cm) that surrounded the reactor, and the sample valves were fixed within. The oven was designed with a maximum operating temperature of 350 °C. The temperature was controlled by an Omega temperature controller. The Micro-reactor was made of stainless steel, with a length of 150 mm and an inside diameter of 6.4 mm, and was surrounded by a brass block, which was itself surrounded by a mica band heater. The reactor was fixed inside the oven, and the reactor temperature was measured using a thermocouple touching the reactor wall.

The reaction products exiting the reactor were analyzed using gas chromatography (Shimadzu AS2010). All gases and the acetic acid were detected using a thermal conductivity detector, TCD. A Porapak Q 80/100 column and Carboxen-1000 column were used as the separation columns with He as the carrier gas.

Result and Discussion

Catalyst Characterization

The crystalline properties of the prepared nano-Pd samples were investigated via X-ray Diffraction (XRD). A typical XRD pattern resulted is shown in Fig. (2). The two prominent peaks for PEG (at 2θ = 19.2^0 and 23.4^0) appeared, indicating the presence of pure polymer. Additionally, the characteristic peak of Pd was obtained.

Pd^0 diffraction lines at 2θ = 39.9^o and 42.9^o are well recognized in X-ray diffractograms.

Transmission electron microscope (TEM) analyses illustrate the presence of a narrow size distribution of the palladium nanoparticles. Fig. (3) Presents the TEM image of the palladium nanoparticles having an average size of approximately 15 nm, which were prepared at 120°C and 2 h using a PEG4600.

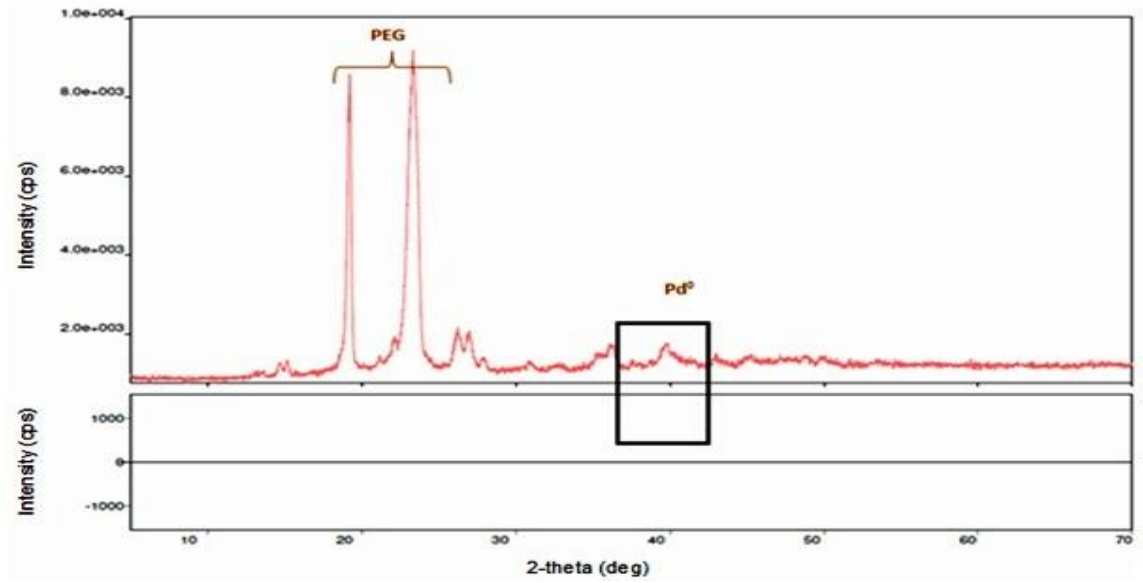

Fig. 2: The XRD pattern of the synthesized Pd-nanoparticles in the polyethylene glycol (PEG) matrix.

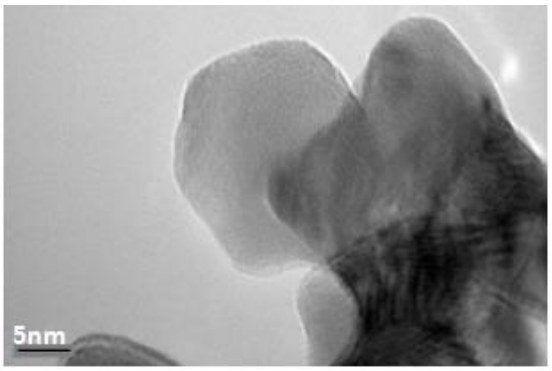

Fig. 3: TEM images of Pd nanoparticles prepared at 120°C for 2 hrs by PEG: $Pd(OAc)_2$ = 4: 0.05 g.

Fig. (4) shows the X-ray diffraction patterns for $Mo_{16}V_{6.37}Nb_{2.05}Pd^0_{0.0037}O_x$ and $Mo_{16}V_{6.37}Nb_{2.05}Pd^0_{0.0037}O_x/TiO_2$. The XRD patterns for the bulk samples resemble those reported previously for similarly prepared bulk samples [3] with a strong line at a 2θ value of 22.58° and weaker lines at 25–30°. These lines have been assigned to the Mo_5O_{14}-like structures that formed when V or Nb substituted into Mo_5O_{14}.[14] The XRD patterns for $Mo_{16}V_{6.37}Nb_{2.05}Pd^0_{0.0037}O_x/TiO_2$ also resembled those reported by Li and Iglesia [11] having strong lines for the anatase and rutile forms of the TiO_2 support and a weak line at 22.58° for the Mo_5O_{14}-like structures.

Ethane Oxidation in the Presence of Nano-Palladium as Co-Catalyst

The oxidation of ethane on $Mo_{16}V_{6.37}Nb_{2.05}O_x$ and $Mo_{16}V_{6.37}Nb_{2.05}O_x$ /TiO_2 resulted in an acetic acid selectivity of approximately 40% and an ethylene selectivity of more than 48% in the best conditions. Thus, the incorporation of the catalytic functions required for ethane oxidation are also required for acetic acid to achieve a higher acetic acid selectivity. The present study focuses on the discussion of ethane oxidation in the presence of nano-Pd. The effect that metallic and oxidized nano-palladium has on Mo-V-Nb oxides was examined to determine the optimum content of each component to achieve the highest acetic acid selectivity. Notably, most catalysts produced increases in the conversion of oxygen with an increase in the amount of added Pd. It is also seen that for all catalysts, increasing the oxygen conversion was accompanied by a decrease in the ethylene selectivity and an increase in the selectivity of both acetic acid and carbon oxides. These variables are related, in that some oxygen was consumed in the ethylene oxidation to produce acetic acid and/or CO_x. This explains why a large change in the oxygen conversion occurred when only a slight change in the ethane conversion took place. Ethane is oxidized to produce both ethylene and acetic acid. The presence of the Pd-based co-catalyst did not influence the ethane oxidation rate but markedly increased the acetic acid synthesis rate by converting the ethylene intermediate to acetic acid. The acetic acid selectivity increased from ~ 40% to ~75%; meanwhile, the ethylene selectivity decreased from ~ 66% to near-complete depletion from the reactor effluent. As reported during the ethylene oxidation, the addition of Pd only increased the rate of the ethylene oxidation forming acetaldehyde, and the active Mo-V-Nb oxides scavenged the acetaldehyde, reacting rapidly to form acetic acid [10, 11].

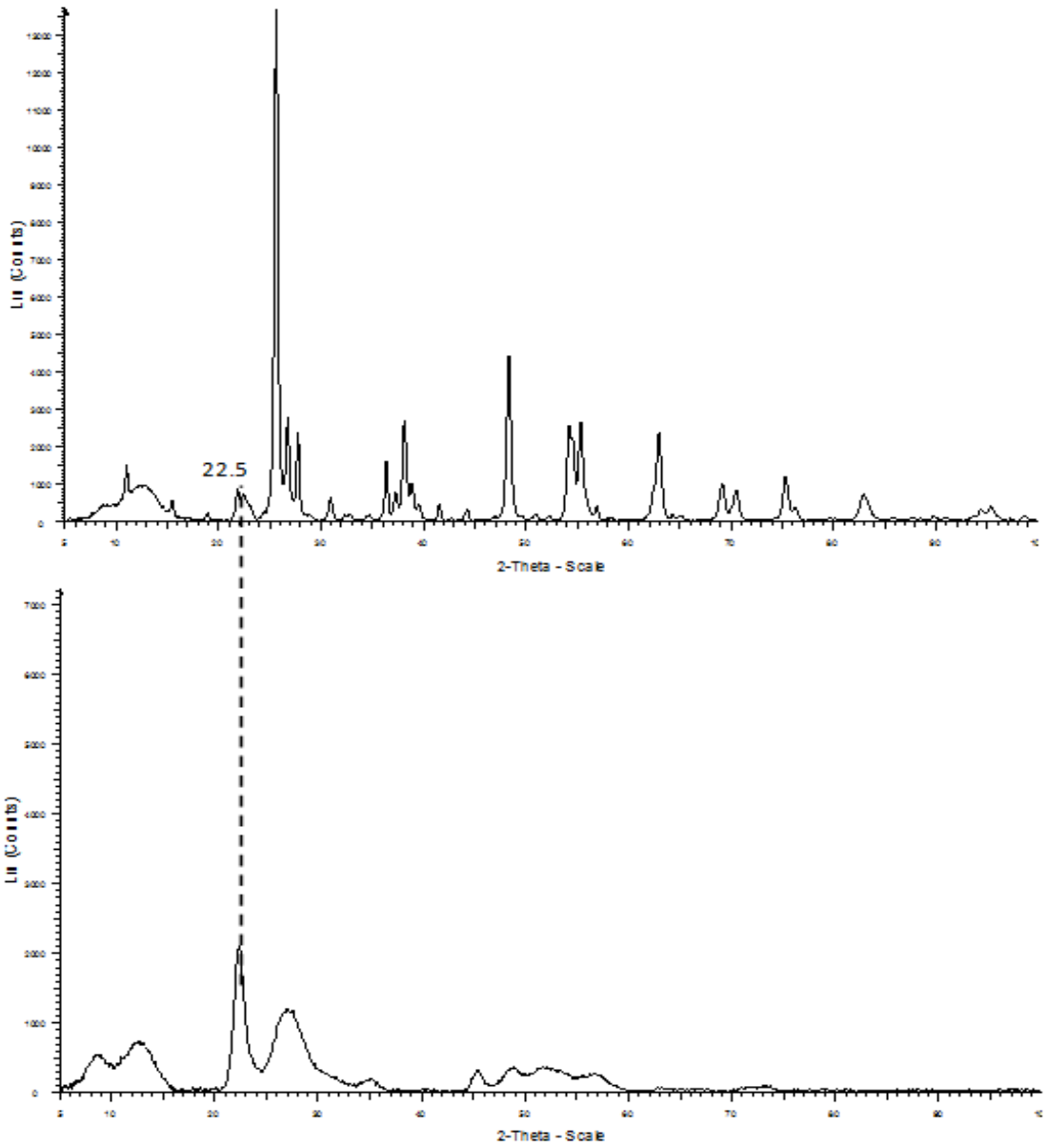

Fig. 4: XRD patterns of $Mo_{16}V_{6.37}Nb_{2.05}Pd^{0}_{0.0037}O_x/TiO_2$ (top) and $Mo_{16}V_{6.37}Nb_{2.05}Pd^{0}_{0.0037}O_x$ (bottom).

Optimum Loading of Nano-PdO_X

To determine the optimum palladium loading, different amounts of nano-palladium were added.

Supported Mo-V-Nb over P25 was promoted with different amounts of nano-PdO_X. Six different catalysts were prepared using different nano-palladium oxide loading percentages (0.000625%, 0.00625%, 0.0125%, 0.025%, 0.034%, and 0.05%). The source of palladium was 10% oxidized palladium on activated charcoal. Ethane oxidation over these catalysts was carried out at reaction temperatures of 220°C and 240°C, at a total pressure of 200 psi with a 15 ml/min feed flow rate. The results are shown in Fig. (5-9).

We found that the activity of the catalysts increased as the nano-palladium oxide loading increased, and this trend was clear in the range below 0.0125%. At 240 °C, the highest values of ethane and oxygen conversion were recorded at 0.0125% loading ($Mo_{16}V_{6.37}Nb_{2.05}Pd_{0.011}Ox/TiO_2$) with values of 8.5% and 84.5%, respectively. The high activity of $Mo_{16}V_{6.37}Nb_{2.05}Pd_{0.011}Ox/TiO_2$ influenced the acetic acid selectivity, demonstrating the highest selectivity and yield among the different loadings. It exhibited

an acetic acid selectivity and yield of 78.4% and $6.66x10^{-2}$, respectively. This selectivity is similar to what has been reached by other investigators. Linke *et al.*. [8] obtained an acid selectivity of 80% and a yield of $2.0x10^{-2}$ when ethane oxidation was carried out on an unsupported Mo-V-Nb catalyst in the presence of bulk Pd; whereas, Borchert *et al.*. [7] obtained 78% and 7.8 $x10^{-2}$. Karim *et al.*. [6] studied the oxidation of ethane on active Mo-V-Nb supported over Al_2O_3, and they reported 84.5% and 5.6 $x10^{-2}$ for the selectivity and yield of acetic acid, respectively. A high selectivity of acetic acid for the oxidation of ethane on $MoVNb/TiO_2$ was obtained by Li and Iglesia [10] who recorded 82% and 4.18 $x10^{-2}$ acetic acid selectivity and yield, respectively.

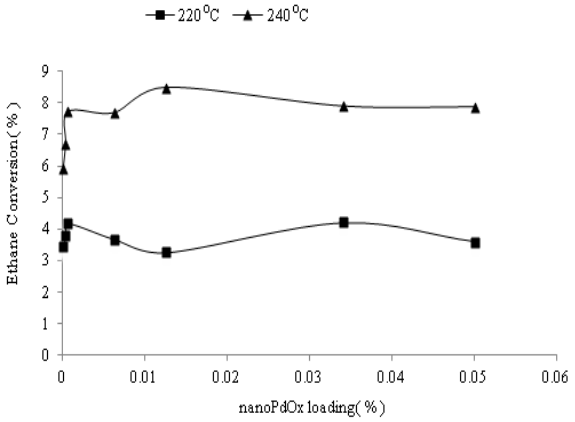

Fig. 5: The nano-PdO_x loading effects on the ethane conversion for a $Mo_{16}V_{6.37}Nb_{2.05}Pd_lO_x/TiO_2$ (P25) catalyst under the reaction conditions of 220 and 240°C, 200 psi and 15 ml/min.

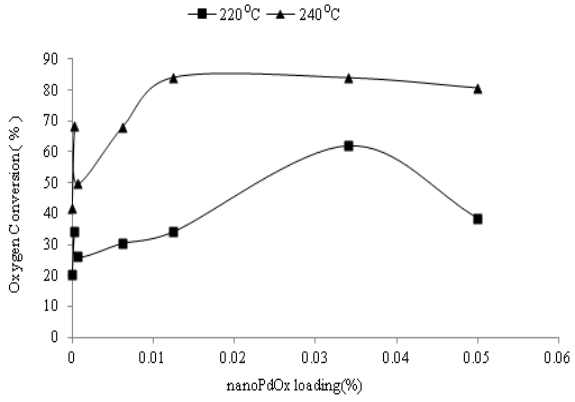

Fig. 6: The nano-PdO_x loading effect on the oxygen conversion for a $Mo_{16}V_{6.37}Nb_{2.05}Pd_lO_x/TiO_2$ (P25) catalyst under the reaction conditions of 220 and 240°C, 200 psi and 15 ml/min.

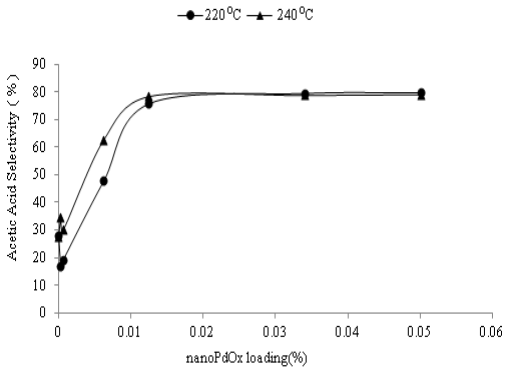

Fig. 7: The nano-PdO_x loading effect on the acetic acid selectivity for a $Mo_{16}V_{6.37}Nb_{2.05}Pd_lO_x/TiO_2$ (P25) catalyst under the reaction conditions of 220 and 240°C, 200 psi and 15 ml/min.

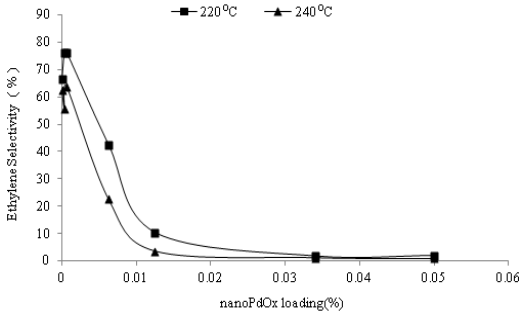

Fig. 8: The nano-PdO_x loading effects on the ethylene selectivity of a $Mo_{16}V_{6.37}Nb_{2.05}Pd_lO_x/TiO_2$ (P25) catalyst under the reaction conditions of 220 and 240 °C, 200 psi and 15 ml/min.

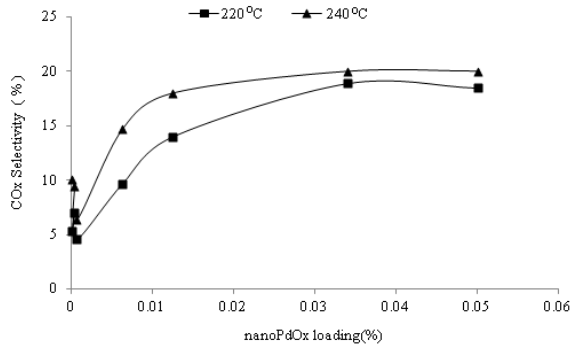

Fig. 9: The nano-PdO_x loading effect on the carbon oxides selectivity of a $Mo_{16}V_{6.37}Nb_{2.05}Pd_lO_x/TiO_2$ (P25) catalyst under the reaction conditions of 220 and 240 °C, 200 psi and 15 ml/min.

From these investigations, we can conclude that 0.0125% is the optimum loading of nano-

palladium oxides for the oxidation of ethane to acetic acid.

Optimum Loading of Metallic Nano-Palladium

Metallic palladium is a well-known catalyst for many chemical reactions. Thus metallic nano-palladium will be examined as the co-catalyst for ethane oxidation over a $Mo_{16}V_{6.37}Nb_{2.05}O_x$ catalyst.

Among the preparations of nano-palladium particles, the chemical reduction of palladium salt in an aqueous or organic solution by suitable reducing agents has been widely adopted. The employment of polymers as reducing agents was mainly involved with the protection of nano-sized palladium from aggregation. Reports of other properties of the polymer, such as the reduction properties, were extremely rare. Polyethylene glycols (PEGs) are inexpensive polymers and widely applied as promising soluble polymeric supports [13]. Herein, we will adopt a novel and facile route that is reported by Luo *et al.*. [13] for the preparation of metallic nano-palladium by exploiting PEG, which was found to act as both a reducing agent and a stabilizer. Because the average molecular weight of PEG influences the fabrication of Pd^0, different molecular weights of polyethylene glycol will be tested.

The preparation of nano-palladium was very straightforward. $Pd(OAc)_2$ was added to the PEG at 120°C in a beaker by magnetic stirring. The resulting homogenous solution was maintained at 120°C with further stirring for 2 h. This resulted in the conversion of the transparent solution to the characteristic gray black color of nano-Pd. The crystalline properties of the prepared samples were investigated using an X-ray Diffraction (XRD). The result of a typical XRD pattern was shown earlier in Fig. (2). The two prominent peaks of polyethylene glycol (at 2θ = 19.2° and 23.4°) was obtained in this pattern, indicating the presence of pure polymer; additionally, the characteristic peak of Pd was obtained.

$Mo_{16}V_{6.37}Nb_{2.05}O_x$ on Degussa P25 was prepared in the presence of metallic nano-palladium. More than six catalysts were prepared with different nano-Pd loading amounts (0.00143%, 0.00285%, 0.00417%, 0.075%, 0.0125%, and 0.05%), and they were tested at 220-240 °C at a total pressure of 200 psi. The results are shown in Fig. (10-14).

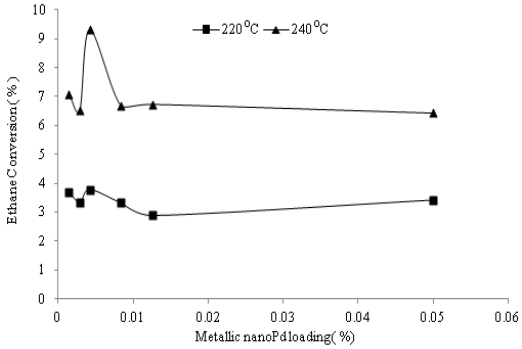

Fig. 10: The ethane conversion as a function of the metallic nano-Pd loading for the oxidation of ethane over $Mo_{16}V_{6.37}Nb_{2.05}Pd_x/TiO_2$(P25) at 220 and 240°C, 200 psi total pressure, and 15 ml/min.

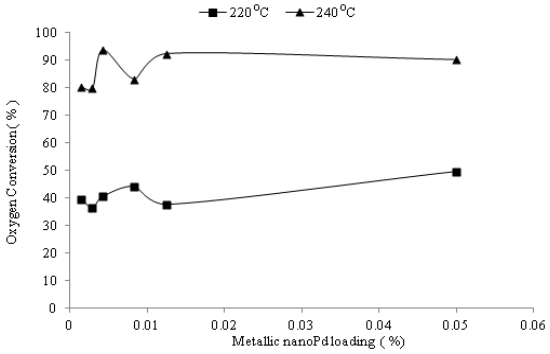

Fig. 11: The oxygen conversion as a function of the metallic nano-Pd loading for the oxidation of ethane over $Mo_{16}V_{6.37}Nb_{2.05}Pd_x/TiO_2$(P25) at 220 and 240°C, 200 psi total pressure, and 15 ml/min.

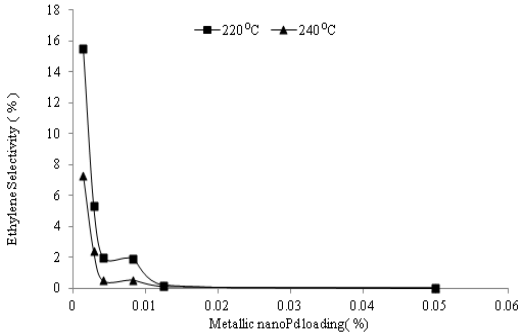

Fig. 12: The ethylene selectivity as a function of the metallic nano-Pd loading for the oxidation of ethane over $Mo_{16}V_{6.37}Nb_{2.05}Pd_x/TiO_2$(P25) at 220 and 240°C, 200 psi total pressure, and 15 ml/min.

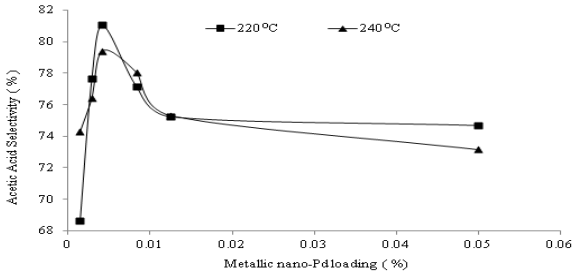

Fig. 13: The acetic Acid selectivity as a function of the metallic nano-Pd loading for the oxidation of ethane over $Mo_{16}V_{6.37}Nb_{2.05}Pd_x/TiO_2$(P25) at 220 and 240°C, 200 psi total pressure, and 15 ml/min.

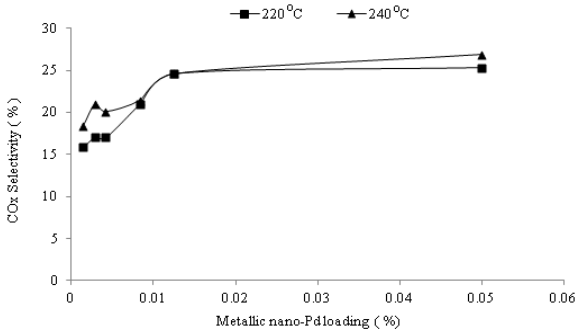

Fig. 14: The CO_x selectivity as a function of the metallic nano-Pd loading for the oxidation of ethane over $Mo_{16}V_{6.37}Nb_{2.05}Pd_x/TiO_2$(P25) at 220 and 240°C, 200 psi total pressure, and 15 ml/min.

It is clear that the catalyst with a 0.00417% nano-palladium loading showed the highest acetic acid selectivity and yield at 9.31% for ethane conversion at a reaction temperature of 240°C. We found that for the Pd loading of 0.00417%, the acetic acid selectivity was 79.42% with a yield of $7.39x10^{-2}$. We can conclude that the optimum loading of metallic nano-palladium for the highest acetic acid productivities is 0.00417%.

This is approximately one third of what we obtained with oxidized Pd.

Effect of Catalyst Loading

In this section, the catalyst with the optimum loading of metallic nano-palladium was supported with different loadings on P25 titania. The catalyst was tested for 5%, 15%, 30%, 50%, 75% and 100% loadings. The experimental results are shown in Fig. (15-17). The total supported catalyst weight in all experiments is 1.0 g. Hence, a 30% loading would mean that the active catalyst weight is 0.3 g. Therefore, the best indicator of the catalyst performance is the space time yield of acetic acid (STY), which is shown in Fig. (17). The graph indicates that the optimum loading is approximately 30%. Three different catalyst loadings were selected for x-ray diffraction analysis. Fig. (18) shows the x-ray diffraction patterns for 15%, 30% and 50% nano-Pd loading. It is clear that there are no extra peaks in any of the materials, indicating that there is no change in the crystal structure of the TiO_2.

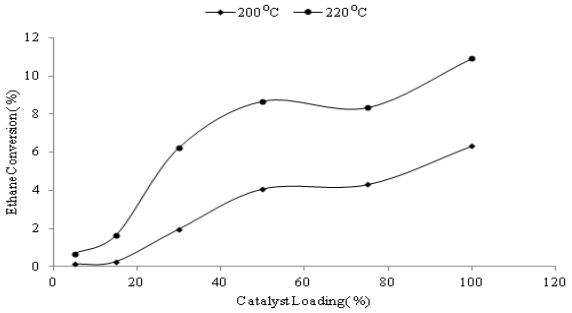

Fig. 15: The ethane conversion as a function of the catalyst loading for the oxidation of ethane on $Mo_{16}V_{6.37}Nb_{2.05}O_x$ $Pd^0_{0.0037}$ /TiO_2 at 200 and 220°C,200 psi and F/W =15 ml/min.g.cat.

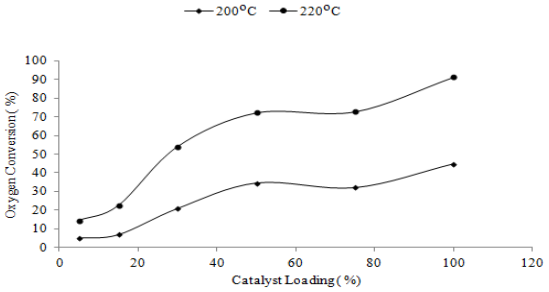

Fig. 16: The oxygen conversion as a function of the catalyst loading for the oxidation of ethane on $Mo_{16}V_{6.37}Nb_{2.05}O_x$ $Pd^0_{0.0037}$ /TiO_2 at 200 and 220°C, 200 psi and F/W =15 ml/min.g.cat.

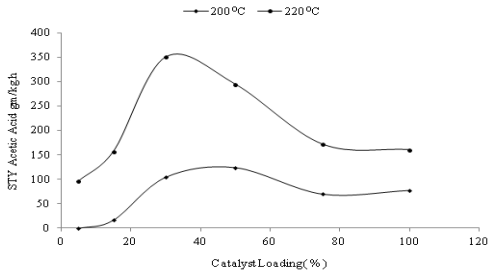

Fig. 17: The space time yield of acetic acid as a function of the catalyst loading for the oxidation of ethane on $Mo_{16}V_{6.37}Nb_{2.05}O_x$ $Pd^0_{0.0037}$ /TiO_2 at 200 and 220°C, 200 psi and F/W =15 ml/min.g.cat.

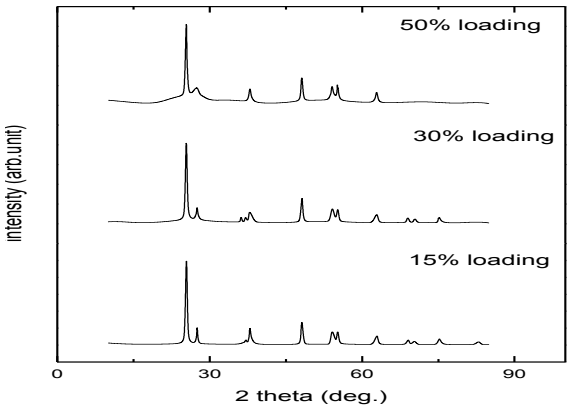

Fig. 18: The X-ray diffraction patterns of the catalysts with 15, 30 and 50% loading on TiO_2.

Other grades of titania from CRISTAL, Aldrich and BDH were less successful.

Effect of Reaction Temperature on the Optimum Catalyst Performance

The effect of the reaction temperature of the ethane oxidation over the best performing catalyst (MoVNb on a P25 support with the optimum nano-palladium loading of 0.00417%, having the formula: $Mo_{16}V_{6.37}Nb_{2.05}O_xPd^0_{0.0037}/TiO_2$) was investigated. The temperatures used in this study were: 200, 220, 230 and 240°C at a total pressure of 200 psi. The total feed flow rate was maintained at 15 ml/min with the percent ethane and oxygen as 82 and 12.5%, respectively. The results are shown in Fig. (19-21).

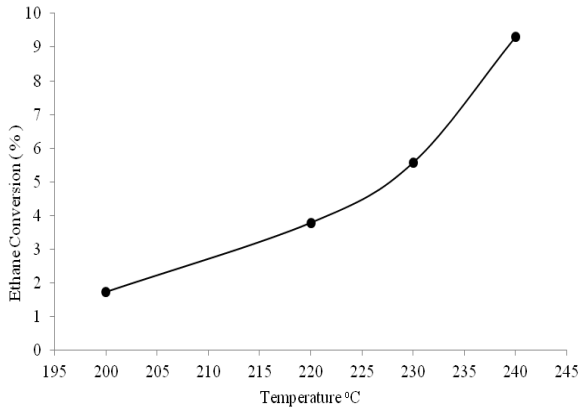

Fig. 19: The ethane conversion as a function of the reaction temperature for the oxidation of ethane on a $Mo_{16}V_{6.37}Nb_{2.05}O_xPd^0_{0.0037}$ /TiO_2 (P25) catalyst at 200 psi and F/W =15 ml/min.g.cat.

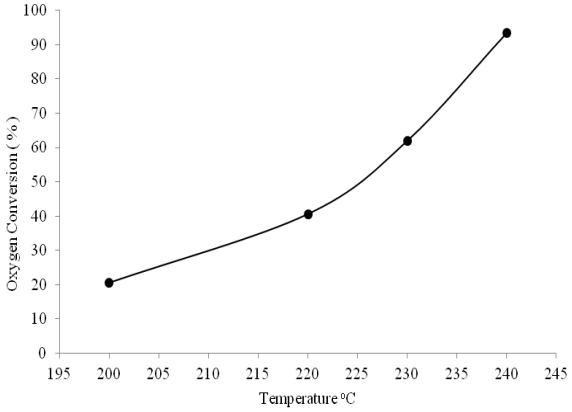

Fig. 20: The oxygen conversion as a function of the reaction temperature for the oxidation of ethane on a $Mo_{16}V_{6.37}Nb_{2.05}O_x$ $Pd^0_{0.0037}$ /TiO_2 (P25) catalyst at 200 psi and F/W =15 ml/min.g.cat.

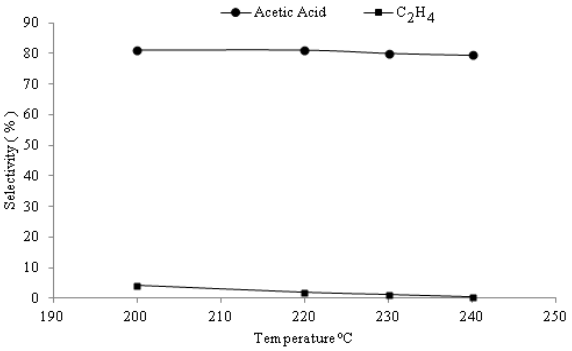

Fig. 21: The acetic acid and ethylene selectivities as function of the reaction temperature for the oxidation ethane on a $Mo_{16}V_{6.37}Nb_{2.05}O_x$ $Pd^0_{0.0037}$ /TiO_2 (P25) catalyst at 200 psi and F/W =15 ml/min.g.cat.

Fig. (19 and 20) show the ethane and oxygen conversions as a function of the reaction temperatures. For each curve, the conversions exponentially increased at high reaction temperatures. For instance, the ethane and oxygen conversions increased from 1.72% and 20.45% at 200°C to 9.31% and 93.55% at 240°C, respectively. It is evident that as the temperature increased, the chemical reaction step also increased. The ethylene selectivity decreased with increasing reaction temperatures as a result of its subsequent conversion to acetic acid and CO_x; meanwhile, the acetic acid selectivity remained relatively constant due to a balance between its formation and its secondary conversion to CO_x. The observed change in the acetic acid and ethylene selectivity with increasing temperature also implies different apparent energies of activation for the direct formation of acetic acid

from ethane (the preferred mechanism at high temperature) and the formation via ethylene (the preferred mechanism at low temperature). That is, the activation energy of the oxidation of ethane to ethylene has to be lower than the activation energy of the direct oxidation of ethane to acetic acid. The carbon oxide selectivity increased with increasing reaction temperature indicating the unselective oxidation reaction of ethane, acetic acid, and ethylene at high reaction temperatures.

Effect of flow rate on the Optimum Catalyst Performance

Experiments were carried out to analyze the influence of the contact time on the reactant conversion and product selectivity. First, 0.2 g of $Mo_{16}V_{6.37}Nb_{2.05}O_xPd^0_{0.0037}/TiO_2$ (P25) catalyst was charged in the reactor at T=275 °C and a constant partial pressure of ethane and oxygen. The changes in the ethane conversion as well as the product selectivity and yield with the feed flow rate are described in Fig. (22-24). At a high flow rate and, thus, a short contact time, ethylene formed with a high selectivity and demonstrated a maximum selectivity of 19.04% as well as a maximum yield of $0.4x10^{-2}$ at a 45 ml/min feed flow rate. At a lower flow rate and, thus, a longer contact time, the ethylene selectivity decreased sharply as a result of its subsequent conversion to acetic acid and CO_x. At high contact times, acetic acid and CO_x resulted as the main products of the ethane oxidation. Ethylene was only formed in trace amounts (S_{C2H4} < 2%); whereas, acetic acid reached a maximum selectivity of 82.03% and a maximum yield of $8.19x10^{-2}$ at a 9.98% ethane conversion. This might result from the residence time of ethylene inside the catalyst bed, wherein, at higher flow rates, the ethylene intermediate did not have time to be significantly converted to acetic acid and CO_x. However, at lower flow rates, the intermediate role of ethylene was clearly demonstrated during the oxidation of ethane in which the residence time increased, and it was nearly depleted from the reactor effluent.

Effect of Preparation Sequence Steps

It is known that the preparation method greatly influences the catalyst properties [15]. Some changes to the preparation method were carried out to enhance the activity of the Mo-V-Nb system towards acetic acid formation. One of these modifications was the rearrangement of the addition of niobium oxalate. As reported, the presence of niobium stabilizes the catalyst structure against oxidation and reduction and permits a very strongly oxidized or reduced catalyst to return more readily to its original state [1]. Herein, we tested what occurs when niobium is added after the addition of titania.

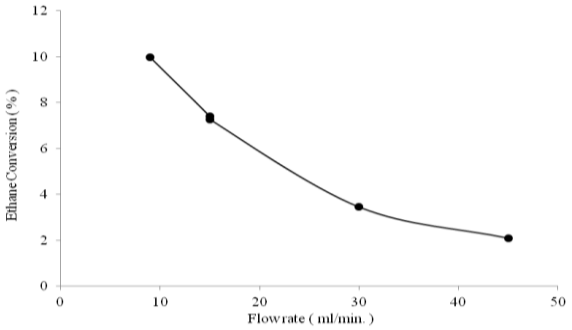

Fig. 22: The ethane conversion as a function of the feed flow rate for the oxidation of ethane on a $Mo_{16}V_{6.37}Nb_{2.05}O_x$ $Pd^0_{0.0037}$ /TiO_2 (P25) catalyst at 275°C and 200 psi.

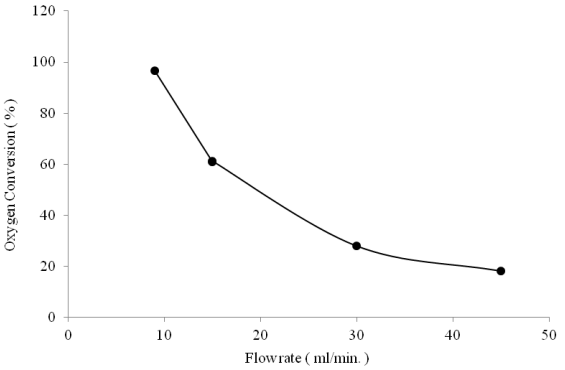

Fig. 23: The oxygen conversion as a function of the feed flow rate for the oxidation of ethane on $Mo_{16}V_{6.37}Nb_{2.05}O_x$ $Pd^0_{0.0037}$ /TiO_2 (P25) catalyst at 275°C and 200 psi.

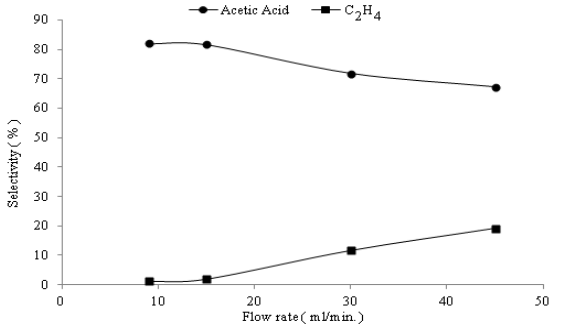

Fig. 24: The ethylene and acetic acid selectivities as a function of the feed flow rate for the oxidation on a $Mo_{16}V_{6.37}Nb_{2.05}O_x$ $Pd^0_{0.0037}$ /TiO_2 (P25) catalyst at 275°C and 200 psi.

Fig. (25-28) show the test results of $Mo_{16}V_{6.37}Nb_{2.05}O_x$ $Pd^0_{0.0037}$ /TiO_2 (P25) with and without the change in the order of the Nb addition under the same catalyst conditions (200 psi, 15 ml/min). It is clear that the acetic acid selectivity increased from 79.42% at a 9.31% ethane conversion to 84.37 at an 11.07% ethane conversion under the same reaction temperature. Therefore, the acetic acid yield increased to a $9.34x10^{-2}$ yield at 240°C. On the other hand, the selectivity of the unselective products (CO_x) decreased from the range of 14.8-20.1% to the range (8.9-15.2%) with preparation change.

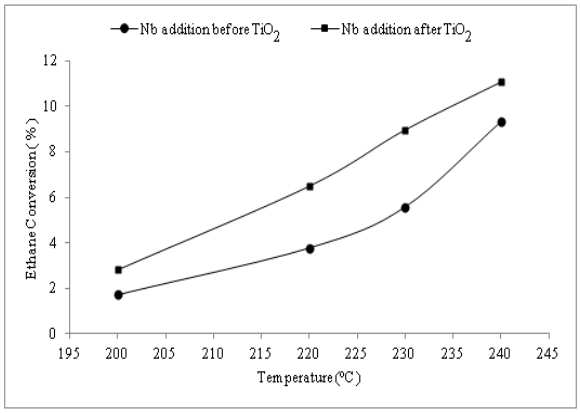

Fig. 25: The ethane conversion as a function of the reaction temperature for the oxidation of ethane on a $Mo_{16}V_{6.37}Nb_{2.05}O_x$ $Pd^0_{0.0037}$ /TiO_2 (P25) catalyst at 200 psi and F/W =15 ml/min.g.cat.

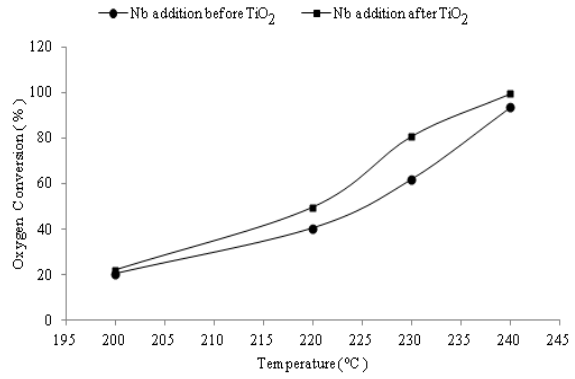

Fig. 26: Oxygen conversion as a function of the reaction temperature for the oxidation of ethane on a $Mo_{16}V_{6.37}Nb_{2.05}O_x$ $Pd^0_{0.0037}$ /TiO_2 (P25) catalyst at 200 psi and F/W =15 ml/min.g.cat.

Durability Study of $Mo_{16}V_{6.37}Nb_{2.05}O_xPd^0_{0.0037}$ /TiO_2 (P25) Catalysts

The stability of the $Mo_{16}V_{6.37}Nb_{2.05}O_xPd^0_{0.0037}$ /TiO_2 (P25) catalyst was tested at 240°C and 200 psi for 75 h with no signs of deactivation. Fig. (29) shows the result.

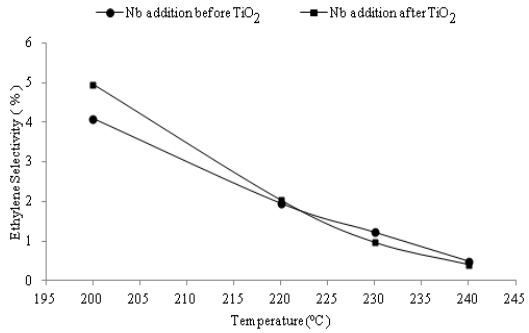

Fig. 27: Ethylene selectivity as a function of the reaction temperature for the oxidation of ethane on a $Mo_{16}V_{6.37}Nb_{2.05}O_x$ $Pd^0_{0.0037}$/TiO_2 (P25) catalyst at 200 psi and F/W =15 ml/min.g.cat.

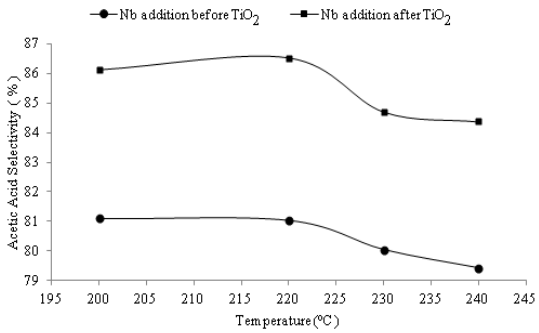

Fig. 28: Acetic acid selectivity as a function of the reaction temperature for the oxidation of ethane on a $Mo_{16}V_{6.37}Nb_{2.05}O_x$ $Pd^0_{0.0037}$ /TiO_2 (P25) catalyst at 200 psi and F/W =15 ml/min.g.cat.

The addition of niobium is known to enhance the intrinsic activity of the MoV combination and improves the selectivity to ethylene by inhibiting the total number of oxidation sites on the catalyst [16]. It seems that Nb also inhibits the total number of oxidation sites of titania, as evidenced by the importance of adding Nb after the addition of titania.

The Pd to V ratio used by Linke *et al.* [8] was 1: 500, and Li and Iglesia [10] tried ratios of 1:600, 1:1200 and 1:2400 with the best results at 1:600. In this work, we found that the optimum ratio for oxidized Pd and metallic Pd is approximately 1:600 and approximately 1:1700, respectively.

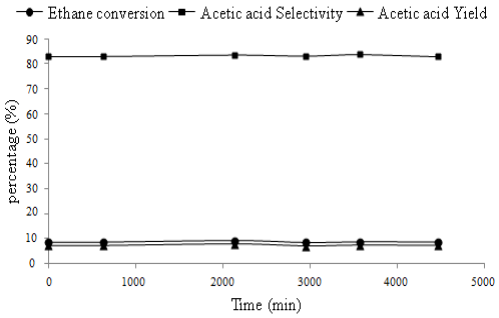

Fig. 29: Ethane conversion, acetic acid selectivity and yield as a function of time for the oxidation of ethane on a $Mo_{16}V_{6.37}Nb_{2.05}O_x$ $Pd^0_{0.0037}$ /TiO_2 (P25) catalyst at 200 psi and F/W =15 ml/min.g.cat.

Li and Iglesia [10] claimed that the use of a physical mixture of Pd/SiO_2 and a M-O-V-Nb catalyst will lead to the efficient use of Pd without limiting accessibility and affecting the catalyst structure. The results of this work do not support this claim. There is no apparent difference between the addition of Pd as a physical mixture and its introduction during catalyst preparation. To explain the increase in the acetic acid productivity in contrast to the decrease in the unselective products, the roles of the active components on the Mo-V-Nb/TiO_2 catalyst should be roughly understood. The selectivity of the unselective products appear to be related to the presence of the exposed support surface linkages Ti-O-Ti or the unselective active components linkages V-O-Ti. These linkages catalyze the oxidation of ethane, ethylene and acetic acid towards carbon oxides. The MoO_x domains are essentially unreactive in the oxidation of ethane, but the presence of MoO_x as well as VO_x in the MoVNb/TiO_2 catalyst led to a marked decrease in the number of exposed V-O-Ti or Ti-O-Ti linkages. The MoO_x in Mo-V-Nb/TiO_2 catalysts caused slightly higher ethylene and acetic acid selectivity, apparently because MoO_x species titrate unselective Ti-O-Ti or V-O-Ti sites and form more selective yet less reducible V-O-Mo linkages. Thus, the addition of niobium after titania might help increase the selective linkages between the active components and the supported surface, which are stabilized in the presence of niobium. Additionally, niobium may play a role in decreasing the undesirable linkages between the support surface and the active components toward increasing the selective linkages.

According to recent works [8, 9 and 17] the yield of acetic acid could be improved by the co-precipitation of noble metals and/or the support of a Mo-V-Nb oxide with Mo_5O_{14}-like structures on TiO_2

The formation of acetic acid was related to the presence of V and Nb-doped Mo_5O_{14}, i.e., $(VNbMo)_5O_{14}$ [15, 16] Pd was said to be responsible for the oxidation of ethylene to acetic acid in a Wacker-like process [8-11]. The shape and size of nano-Pd can be controlled, as shown by Lim *et al.*. [18]. This creates more research pathways for improving the acetic acid yield.

Conclusions

By supporting the catalyst $Mo_{16}V_{6.37}Nb_{2.05}O_x$ on Degussa P25 titania, the catalyst selectivity towards acetic acid improved. The effect of the catalyst loading over the Titania (P25) was studied, and the optimum loading was found to be approximately 30%.

Ethane oxidation in the presence of either nano-palladium oxides or metallic nano-palladium showed shifts in the reaction towards acetic acid formation. The presence of nano-PdO_x or a nano-Pd^0-based co-catalyst did not influence the ethane oxidation rates, but markedly increased the acetic acid synthesis rates by converting the ethylene intermediates to acetic acid. For both sources of nano-palladium, a high value of selectivity for acetic acid occurred in which ethylene was nearly depleted from the reactor effluent. The optimum loading of nano-PdO_x and of nano-Pd^0 was recorded at 0.0125% and 0.00417%, respectively.

The optimum amount of metallic nano-Pd loading was approximately one third of that of oxidized Pd.

The acetic acid selectivity increased from 79.91% at a 9.31% ethane conversion (with an acetic acid yield of $7.394x10^{-2}$) to a selectivity of 84.37% at an ethane conversion of 11.07% (with an acetic acid yield of $9.34x10^{-2}$) at the same reaction temperature (240°C) when the order of the addition of the niobium oxalate solution was changed from before the addition of titania to after.

The influence of the reaction temperature on the catalytic activity of the partial oxidation of ethane on $Mo_{16}V_{6.37}Nb_{2.05}NanoPd^0_{0.0037}$ was studied. The observed change in the acetic acid and ethylene selectivity with increasing temperature implies different apparent energies of activation, with the direct formation of acetic acid from ethane preferred at high temperature and the formation via ethylene preferred at low temperature.

The ethylene selectivity decreased strongly with increasing contact time, as a result of its subsequent

conversion to acetic acid and CO_x, and they emerge as the main products of the ethane oxidation.

According to recent works [8, 9 and 17] the yield of acetic acid could be improved by the co-precipitation of noble metals and/or the support of a Mo-V-Nb oxide with Mo_5O_{14}-like structures on TiO_2

The stability of $Mo_{16}V_{6.37}Nb_{2.05}O_x$ $Pd^0_{0.0037}/TiO_2$ was tested for more than 75 h. The catalytic activity remained constant with the passage of time.

Acknowledgement

The authors acknowledge the financial support provided by King AbdulAziz City for Science and Technology (KACST) for this research under grant number AR-29-256.

References

1. E. M. Thorsteinson, T. P. Wilson, F. G. Young and P. H. Kasai, The Oxidative Dehydrogenation of Ethane over Catalysts Containing Mixed Oxides of Molybdenum and Vanadium, *J. Catal.***, 52**, 116 (1978).
2. K. Sano, H. Uchida and S. Wakabayashi, A New Process for Acetic Acid Production by Direct Oxidation of Ethylene, *Catal. Surv. Jpn.***, 3**, 55 (1999).
3. F. G. Young and E. M. Thorsteinson, Low Temperature Oxydehydrogenation of Ethane to Ethylene, U.S. Patent **4**, 250, 346 (1981).
4. K. Karim, E. Mamedov, M. H. Al-Hazmi, A. H. Fakeeha, M. A. Soliman, Y. S. Al-Zeghayer, A. S. Al-Fatish and A. A. Al-Arify, Catalysts for Producing Acetic Acid from Ethane Oxidation Proceses for Making Same and Method of Using Same, U.S. Patent 6, 030, 920, Feb 29 (2000).
5. K. Karim, E. Mamedov, M. H. Al-Hazmi, A. H. Fakeeha, M. A. Soliman, Y. S. Al-Zeghayer, A. S. Al-Fatish and A. A. Al-Arify, Catalysts Methods for Producing Acetic Acid from Ethane Oxidation Using MO, V, PD and NB Based Catalysts, Processes of Making Same and Methods of Using Same, U.S. Patent 6, 310, 241, Oct 30 (2001).
6. K. Karim, E. Mamedov, M. H. Al-Hazmi, A. H. Fakeeha, M. A. Soliman, Y. S. Al-Zeghayer, A. S. Al-Fatish and A. A. Al-Arify, Catalysts for Producing Acetic Acid from Ethane Oxidation, Processes of Making Same and Methods of Using Same, U.S. Patent 6, 383, 977, May 7 (2002).
7. H. Borchert and U. Dingerdissen, (Hoechst), Ger.offen.DE Patent 19 630 832 (1998).
8. D. Linke, D. Wolf, M. Baerns, O. Timpe, R. Schlögl, S. Zeyβ and U. Dingerdissen, Catalytic Partial Oxidation of Ethane to Acetic Acid over $Mo_1V_{0.25}Nb_{0.12}Pd_{0.0005}O_x$: I. Catalyst Performance and Reaction Mechanism, *J. Catal.*, **205**, 16 (2002).
9. D. Linke, D. Wolf, M. Baerns, S. Zeyβ and U. Dingerdissen, Catalytic Partial Oxidation of Ethane to Acetic Acid over $Mo_1V_{0.25}Nb_{0.12}Pd_{0.0005}O_x$: II. Kinetic Modelling, *J. Catal.***, 205**, 32 (2002).
10. X. Li and E. Iglesia, Support and Promoter Effects in the Selective Oxidation of Ethane to Acetic Acid Catalyzed by Mo-V-Nb Oxides, *Appl. Catal. A Gen.*, **334**, 339 (2008).
11. X. Li and E. Iglesia, Kinetics and Mechanism of Ethane Oxidation to Acetic Acid on Catalysts Based on Mo−V−Nb Oxides, *J. Phys. Chem.* C, **112,** 15001 (2008).
12. Y. S. Al-Zeghayer, A. S. Al-awadi, B. Y. Jibril, M. A. Soliman and S. Al-Mayman, Partial Oxidation of Ethane to Acetic Acid on Titania Supported MoVNbPd Catalyst, *Asian J. Chem.*, **25**, 7979 (2013).
13. C. Luo, Y. Zhang and Y. Wang, Palladium Nanoparticles in Poly(Ethyleneglycol): the Efficient and Recyclable Catalyst for Heck Reaction, *J. Mol. Catal. A Chem.***, 229**, 7 (2005).
14. P. A. Namini, A. A. Babaluo and B. Bayati, Palladium Nanoparticles Synthesis Using Polymeric Matrix: Poly(Ethyleneglycol) Molecular Weight and Palladium Concentration Effects, *International Journal Nanoscience and Nanotechnology*, **3**, 37 (2007).
15. M. Merzouki, B. Taouk, L. Tessier, E. Bordes and P. Courtine, Correlation between Catalytic and Structural Properties of Modified Molybdenum and Vanadium Oxides in the Oxidation of Ethane in Acetic Acid or Ethylene, *Stud. Surf. Sci. Catal.***, 75**, 753 (1993).
16. O. Desponds, R. L. Keiski and G. A. Somorjai, The Oxidative Dehydrogenation of Ethane over Molybdenum-Vanadium-Niobium Oxide Catalysts: The Role of Catalyst Composition, *Catal. Lett.***, 19**, 17 (1993).
17. M. Roussel, M. Bouchard, E. Bordes-Richard, K. Karim and S. Al-Sayari, MoVO-Based Catalysts for the Oxidation of Ethane to Ethylene and Acetic Acid: Influence of Niobium and/or Palladium on Physicochemical and Catalytic Properties, *Appl. Catal. A Gen.*, **308,** 62 (1993).
18. B. Lim, M. Jiang, J. Tao, P. H. C. Camargo, Y. Zhu and Y. Xia, Shape-Controlled Synthesis of Pd Nanocrystals in Aqueous Solutions, *Adv. Funct. Mater.*, **19**, 189 (2009).